Storage-dependent drainable porosity for complex hillslopes

A. G. J. Hilberts and P. A. Troch

Hydrology and Quantitative Water Management Group, Wageningen University, Netherlands

C. Paniconi

Institut National de la Recherche Scientifique, Centre Eau, Terre et Environnement, Université du Québec, Quebec, Quebec, Canada

Received 1 October 2004; revised 18 February 2005; accepted 15 March 2005; published 2 June 2005.

[1] In hydraulic groundwater theory the parameter drainable porosity f (a storage coefficient that accounts for the effect of the unsaturated zone on water table dynamics) is usually treated as a constant. For shallow unconfined aquifers the value of this parameter, however, depends on the depth to the water table and the water retention characteristics of the soil. In this study an analytical expression for f as a function of water table depth is derived under the assumption of quasi-steady state hydraulic equilibrium, in this way accounting, in part, for the effects of the unsaturated zone on groundwater dynamics. The derived expression is implemented in the nonlinear hillslope-storage Boussinesq (HSB) model (Troch et al., 2003) to simulate the drainage response of complex hillslopes. The model's behavior is analyzed by comparison to (1) the HSB model with a constant value for f and (2) measurements of water tables and outflow hydrographs on a $6.0 \times 2.5 \times 0.5$ m laboratory hillslope experiment. The comparison is conducted for a pure drainage case on two different hillslope shapes (linearly convergent and divergent) and for three different slope inclinations (5%, 10%, and 15%). Comparison 1 is run in an uncalibrated and a fully calibrated mode, and it enables us to evaluate the effect of a dynamic, state-dependent value for f on model output. Comparison 2 allows us to test the HSB model on several hillslope configurations and to analyze whether the concept of a storage-dependent f enhances the model performance. The comparison of the HSB models to the measurements from the laboratory hillslopes shows that it is possible to capture the general features of the outflow hydrograph during a drainage experiment using either one of the HSB models. Overall, the original (constant f) HSB model, with one fitting parameter more than the revised HSB model, shows a slightly better fit on the hydrographs when compared to the revised (variable f) HSB model. However, the peak outflow values (the first few minutes after initiation of the experiments) are better captured by the revised HSB model. The revised HSB model's performance in simulating water table movements is much more accurate than that of the original HSB model. The improved match of the revised HSB model to piezometric measurements is worth stressing because the ability to model water tables is a key attribute of the model, making it possible to investigate phenomena such as saturation excess runoff. Also noteworthy is the good match between the revised HSB model and the outflow measurements, without any calibration, for the divergent slopes. The changing values of the calibrated drainable porosity parameter for the original HSB model as different configurations are simulated (slope angle, plan shape, initial conditions), together with the ability of the revised HSB model to more accurately simulate water table dynamics, clearly demonstrates the importance of regarding drainable porosity as a dynamic, storage-dependent parameter.

Citation: Hilberts, A. G. J., P. A. Troch, and C. Paniconi (2005), Storage-dependent drainable porosity for complex hillslopes, *Water Resour. Res.*, *41*, W06001, doi:10.1029/2004WR003725.

1. Introduction

[2] Within its range of validity, Richards' equation [*Richards*, 1931] provides the most accurate description of flow processes through variably saturated porous media. However, in catchment and hillslope hydrological modeling practices, the application of Richards' equation is generally

0043-1397/05/2004WR003725$09.00

cumbersome due to difficulties in the parameterization of the equation, and due to the typically large computational time that is required for solving the equation. For this reason much research has been devoted to investigating the possibility of using simpler models (analytical and numerical) that still reflect the true physical behavior of a catchment or a part thereof [e.g., *Beven*, 1981; *Stagnitti et al.*, 1986; *Zecharias and Brutsaert*, 1988; *Duffy*, 1996; *Woods et al.*, 1997; *Fan and Bras*, 1998; *Hogarth et al.*, 1999; *Ogden and Watts*, 2000; *Parlange et al.*, 2001; *Troch et al.*, 2002, 2003, 2004; *Paniconi et al.*, 2003; *Hilberts et al.*, 2004]. The drainable porosity parameter (also in some cases referred to as specific yield) is introduced in hydraulic groundwater equations for the purpose of mass conservation, i.e., matching the modelled outflow volumes to groundwater table dynamics, thereby accounting in some way for capillarity and unsaturated zone effects. It is generally treated as a parameter with a constant value. However, studies carried out under nearly saturated conditions [e.g., *Gillham*, 1984; *Abdul and Gillham*, 1989], and preliminary results from our recent experimental work on a laboratory hillslope suggest that this parameter varies in time and space, which indicates the influence of storage dynamics in the unsaturated zone on the hydraulic groundwater model. Moreover, *Paniconi et al.* [2003] and *Hilberts et al.* [2004] (who make comparisons with a three-dimensional Richards based model) show that the water table dynamics and outflow rates are sensitive to this parameter value. The preliminary experimental results mentioned above, and the conclusions from the comparison to a three-dimensional Richards equation based model in the papers motivate us to search for an appropriate (analytical) expression that links the drainable porosity to the state of the (unconfined) aquifer. Our intention is to investigate the possibility of capturing some of the unsaturated zone's influence on groundwater movement by introducing a physically based description of the drainable porosity parameter.

[3] In the literature we find two slightly different definitions of drainable porosity or specific yield for unconfined aquifers. *Johnson* [1967] and *Bear* [1972] define specific yield as the ratio of the volume of water that a saturated rock or soil will yield by gravity to the total volume of the rock or soil (definition 1). These authors consider the yield starting from complete saturation to complete gravitational drainage, and it is thus regarded as an aquifer property. *Luthin* [1966], *Freeze and Cherry* [1979], *Neuman* [1987], and *Dingman* [2002], however, define specific yield as the volume of stored groundwater released per unit area per unit decline of water table (definition 2). This definition implies a parameter that is dependent on the state (water table position) of the system. *Bear* [1972] summarizes by noting that the parameter as under definition 2 is the drainable porosity and is sometimes used to denote the ''instantaneous'' specific yield. In this paper, Bear's definition for drainable porosity as in definition 2 is adopted, and it can therefore be expressed as

$$f = \frac{v}{\triangle h'} \quad (1)$$

where v is the amount of water drained (i.e., drainage volume per unit surface area) [L], and h' is the water table elevation above an arbitrary horizontal datum [L]. The vertical water table height is indicated with a prime because the coordinate system will in this paper be changed to water tables measured perpendicular to the bedrock. Although often treated as such, drainable porosity is not a static soil characteristic: it typically changes during the course of a rainfall or drainage event [e.g., *Tritscher et al.*, 2000; *Moench*, 2003; *Weiler and McDonnell*, 2004; *Szilagyi*, 2004]. It has been reported that the drainable porosity is a function of soil moisture conditions in the unsaturated zone above the water table [*Luthin*, 1966; *Bear*, 1972; *Hillel*, 1980]. More specifically, *Kim and Bierkens* [1995] (in reply to *Su* [1994]) suggested to regard the drainable porosity parameter that was used in a Boussinesq-type model as a function of the groundwater level under the assumption of hydraulic equilibrium conditions in the unsaturated zone. *Bierkens* [1998] linked drainable porosity directly to the depth to the water table for the case of horizontal bedrock. *Nachabe* [2002] put forward the concept that for shallow unconfined aquifers the drainable porosity (i.e., transient or instantaneous specific yield) can be significantly influenced by capillarity effects, especially in early stages of drainage experiments. Other studies that have examined capillary fringe effects on subsurface dynamics, both theoretically and experimentally, include those by *Parlange and Brutsaert* [1987], *Parlange et al.* [1990], *Fink et al.* [2001], *Walter et al.* [2000], and *Nielsen and Perrochet* [2000]. *Nachabe* [2002] describes a relationship between drainable porosity and depth to the water table, including effects of delayed drainage for rapidly moving water tables using a Brooks-Corey parameterization for the unsaturated zone. Except for *Bierkens* [1998] and *Nachabe* [2002], the literature provides little theoretical work that quantitatively links drainable porosity to moisture content, suction head, or water table height. Moreover, the classical techniques and methods to determine drainable porosity experimentally are a topic of discussion. Different methods often lead to results that differ by as much as an order of magnitude in the early stages of drawdown experiments [*Neuman*, 1987; *Nwankwor et al.*, 1992; *Moench*, 1994; *Heidari and Moench*, 1997].

[4] *Tritscher et al.* [2000] showed the dependency of drainable porosity on the degree of saturation under a variety of conditions. Both this study and that of *Nachabe* [2002] draw the conclusion that the drainable porosity can be strongly influenced by water table depth. *Tritscher et al.* [2000] report differences as high as a factor 100 between the drainable porosity values for the deepest versus the shallowest water tables. In view of these previous studies, the question arises as to how varying values of drainable porosity affect the (modelled) water table movements and outflow patterns.

[5] In this paper we first derive an analytical expression for drainable porosity as a function of water table depth. By assuming a vertical hydrostatic soil water pressure distribution in the unsaturated zone, we express drainable porosity as a storage-dependent variable (that is, as a function of water table depth and the hydraulic parameters of the soil) for horizontal and sloping bedrock types. The derived expression is then implemented in the physically based nonlinear ''hillslope-storage Boussinesq'' (HSB) model as developed by *Troch et al.* [2003], *Paniconi et al.* [2003], and *Hilberts et al.* [2004]. This implementation enables us

to test the validity of the derived equation and also allows for an analysis of the effect of variability in the drainable porosity value on the dynamic hydrological behavior of a physically based model. The model results are evaluated by comparing them to (1) the results of the original (constant f) nonlinear HSB model to explicitly assess the effect of storage-dependent drainable porosity and (2) to measurements of water tables and outflow rates on a scaled hillslope laboratory experiment of 6.0 × 2.5 × 0.5 m. By comparison to laboratory measurements we are able to assess whether the HSB model is capable of reproducing water table movements and outflow patterns, and if the concept of storage-dependent drainable porosity offers any advantages in terms of accuracy when compared to the original HSB model.

2. Drainable Porosity and Groundwater Storage

2.1. Storage in the Saturated and Unsaturated Zone for a Horizontal Bedrock

[6] In an unconfined aquifer a drainage event causes the water table to move downward, thereby decreasing the size of the saturated zone and enlarging the unsaturated zone. Consequently, drainage of groundwater can result in a decrease in groundwater level directly and in changes in storage in the unsaturated zone. Assuming there is no recharge, we can define the drainable porosity as the change in total storage with respect to a unit change in water table depth. However, the choice of the length of a "unit change" is undefined and arbitrary. A clearer definition is obtained when taking the limit case in equation (1) of f for $\Delta h' \rightarrow 0$, from which we obtain the expression

$$f(\psi, h') = \frac{\mathrm{d}s}{\mathrm{d}h'} \tag{2}$$

where $\psi = \psi(z)$ is pressure head [L], t is time [T], and $s = s(\psi, h')$ is the total storage of soil moisture [L] (see Figure 1) which can be expressed as:

$$s(\psi, h') = s_1(\psi) + s_2(h') \tag{3}$$

where $s_1(\psi)$ is the total available storage of soil moisture above the water table [L] and $s_2(h')$ is the total available storage of water in the saturated zone [L]. The available soil moisture storage above the water table can be expressed as

$$s_1(\psi) = \int_{h'}^{Z} (\theta(\psi) - \theta_r)\mathrm{d}z \tag{4}$$

where $\theta(\psi)$ is the soil water content (dimensionless), z is the vertical coordinate (positive upward) [L], Z is the location of the ground surface above a horizontal datum, and θ_r is the residual soil moisture content (dimensionless). The integration of (4) is taken over $(Z - h')$ which corresponds to the depth of the unsaturated zone above the water table. The storage of groundwater in the saturated zone is given by:

$$s_2(h') = (\theta_s - \theta_r)(h' - z_0) \tag{5}$$

where z_0 is the height of the bedrock above a given horizontal datum [L] and θ_s is the moisture content at saturation. Note that we implicitly assume that water that is

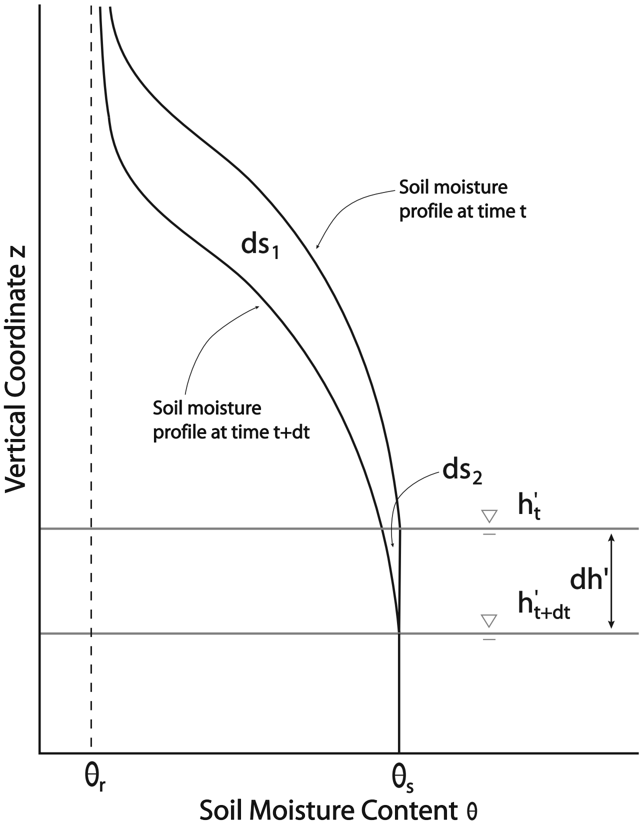

Figure 1. Sketch of hypothetical soil moisture profiles and corresponding changes in saturated and unsaturated storage, in relation to water table depth h' at two time instances (t and t + dt).

released as a result of compressibility of the groundwater and the porous matrix is negligible compared to the water that is released as a result of the emptying of the pore space (i.e., specific storage coefficient is equal to 0).

2.2. Integration of Soil Moisture Curves for a Horizontal Bedrock

[7] To solve (4) we require a relationship between soil moisture content θ and suction head ψ, and a relationship between ψ and z. To solve (2) we need an expression for storage s_1 in terms of water table depth h'. Under the assumption of zero vertical flux, and that the suction head profile changes from one steady state situation to another over the time it takes to impose dh' (quasi-steady state assumption), the relationship between ψ and z is that of hydraulic equilibrium:

$$\psi = h' - z \tag{6}$$

This assumption is valid either when the movement of the water table is relatively slow, so that an equilibrium state can be reached above the water table [*Luthin*, 1966], or for shallow systems where redistribution of soil moisture is rapid [*Bierkens*, 1998]. The constitutive relationship between θ and ψ used in this study is the van Genuchten function [*van Genuchten*, 1980]:

$$\theta(\psi) = \theta_r + (\theta_s - \theta_r)\left\{\frac{1}{1 + (\alpha\psi)^n}\right\}^m \tag{7}$$

where α $[L^{-1}]$, n (>0) (dimensionless), and m (dimensionless) are van Genuchten parameters. Combining (6) and (7) we obtain

$$\theta(h') = \theta_r + (\theta_s - \theta_r)\left\{\frac{1}{1 + (\alpha(h' - z))^n}\right\}^m \quad (8)$$

Troch [1992] found that for the $\theta(\psi)$ relationship it is possible to assume that the relationship between m and n is given by

$$m = 1 + 1/n \quad (9)$$

instead of the more common definition $m = 1 - 1/n$ [e.g., *van Genuchten*, 1980], without losing the ability to aptly fit the soil moisture retention data for a wide range of soil types. Using (8) and (9) in (4), we obtain a simple mathematical expression for the unsaturated zone storage s_1, given the position of the water table h':

$$\begin{aligned} s_1(h') &= \int_{h'}^{Z} \{\theta_s - \theta_r\}\left\{\frac{1}{1 + (\alpha(h' - z))^n}\right\}^m \mathrm{d}z \\ &= (Z - h')(\theta_s - \theta_r)\left(1 + (\alpha(h' - Z))^n\right)^{(-1/n)} \end{aligned} \quad (10)$$

The total storage can now be expressed as

$$\begin{aligned} s(h') &= s_1(h') + s_2(h') \\ &= (Z - h')(\theta_s - \theta_r)\left(1 + (\alpha(h' - Z))^n\right)^{(-1/n)} \\ &\quad + (\theta_s - \theta_r)(h' - z_0) \end{aligned} \quad (11)$$

2.3. Drainable Porosity for a Horizontal Bedrock

[8] The first-order derivative of s with respect to h' yields the drainable porosity (see (2)):

$$f(h') = (\theta_s - \theta_r)\left\{1 - \left(1 + (\alpha(h' - Z))^n\right)^{-\left(\frac{n+1}{n}\right)}\right\} \quad (12)$$

[9] Equation (12) is an analytical expression that relates drainable porosity to local water table depth and is dependent on the soil moisture retention characterization through the van Genuchten parameters. An analogous expression was also derived by *Bierkens* [1998] based on the integration described by *Troch* [1992]. Note that the derived expression assumes zero vertical flux. Generalizing to nonzero fluxes is possible [e.g., *Rockhold et al.*, 1997], although in this case we would not obtain closed form solutions for the storage-dependent drainable porosity.

2.4. Drainable Porosity for a Sloping Bedrock

[10] To implement the derived expression for drainable porosity for horizontal bedrock into Boussinesq-type hillslope models [e.g., *Boussinesq*, 1877; *Troch et al.*, 2003], the coordinate system has to be modified such that the water table depth is taken perpendicular to the bedrock. This can be done by substituting

$$h' - z_0 = \frac{h}{\cos(i)} \quad (13)$$

$$Z - h' = \frac{D - h}{\cos(i)} \quad (14)$$

into (11), where D $[L]$ and $h(x, t)$ $[L]$ are the soil depth and the water table height measured perpendicular to the bedrock and $i = i(x)$ (dimensionless) is the bedrock slope at coordinate x $[L]$ parallel to the bedrock (see Figure 2). From (13) we obtain

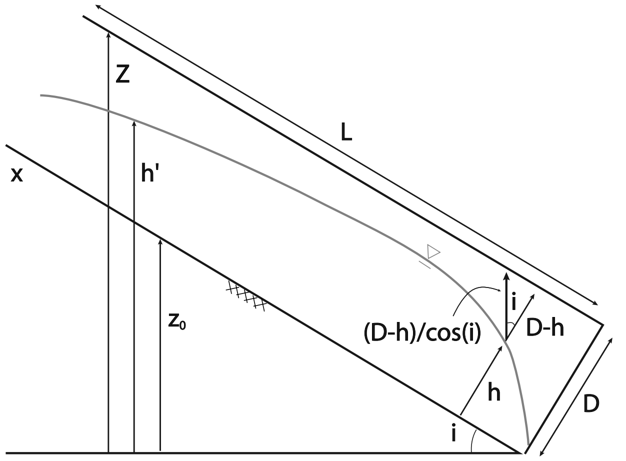

Figure 2. Sketch of a sloping unconfined aquifer with bedrock slope (i), water table elevation h', soil surface elevation Z, and bedrock elevation z_0, together with water table height h, depth to water table ($D - h$), hillslope length (L), and soil depth (D) defined with respect to a reference frame perpendicular to the bedrock and parallel to coordinate x.

$$f(h) = \frac{\mathrm{d}s}{\mathrm{d}h} = \frac{\mathrm{d}s}{\mathrm{d}h'} \cdot \frac{\mathrm{d}h'}{\mathrm{d}h} = \frac{f(h')}{\cos(i)} \quad (15)$$

Substitution of (12), (13), and (14) into (15) yields the expression for drainable porosity that will be implemented into the HSB model:

$$f(h) = (\theta_s - \theta_r)\left\{1 - \left(1 + \left(\alpha\left(\frac{h - D}{\cos(i)}\right)\right)^n\right)^{-\left(\frac{n+1}{n}\right)}\right\} \quad (16)$$

[11] By choosing this coordinate system we thus assume that the saturated zone fluxes are parallel to the bedrock (the extended Dupuit-Forchheimer assumption [*Childs*, 1971]), and that the relationship between outflow and water table fluctuations is characterized by drainable porosity, which in turn is dependent on the water table height and the soil water retention characteristics.

2.5. Interpretation

[12] Under the assumption that leads to (16) (i.e., no recharge and hydrostatic pressure distribution in the unsaturated zone), we can analyze the behavior of this expression. To interpret it let us first analyze the limit values of the function. For shallow unconfined aquifers under humid conditions (i.e., relatively high water tables), h will approach D. This limit case yields:

$$\lim_{h \uparrow D} f(h) = 0$$

For very deep aquifers with deep groundwater tables, D approaches ∞ and therefore:

$$\lim_{D \to \infty} f(h) = \theta_s - \theta_r$$

The drainable porosity for completely saturated soils is very close to 0 because an infinitesimal change in water table location will not result in any outflow, due to the binding of water in the capillary fringe. As the water table drops, the marginal effect of capillarity decreases and as a result drainable porosity values initially increase. This was also noted by *Kim and Bierkens* [1995] and *Nachabe* [2002]. When water tables are deep, a drop in water table will result in a downward shift of the soil moisture profile without a significant change of shape of the profile. Consequently the change in unsaturated storage (ds_1/dh) will then approach 0, and the drainable porosity converges to $ds_2/dh = \theta_s - \theta_r$. In Figure 3 the drainable porosity from equation (16) for a characteristic sand, loam, and clay soil is plotted as a function of the depth to the water table. The van Genuchten parameters used to produce these results are given in Table 1. Figure 3 shows that for nearly saturated conditions drainable porosity for all soil types goes to zero. For deep groundwater tables, the drainable porosity converges asymptotically to $\theta_s - \theta_r$. Because sandy soil has a low retention capacity, and consequently the range in which capillarity has a significant effect on storage is small, the maximum of f is reached relatively quickly (in terms of depth to the water table) in comparison to loam and clay soils.

3. Implementation of Storage-Dependent Drainable Porosity Into the HSB Model

[13] The mass balance equation for a three-dimensional hillslope reads:

$$\frac{\partial S}{\partial t} = -\frac{\partial\{wq\}}{\partial x} + Nw \tag{17}$$

where $w = w(x)$ $[L]$ is the hillslope width at x, N is the recharge to the groundwater table $[LT^{-1}]$, $q = q(h)$ $[L^2T^{-1}]$ is the Darcy flux, and $S = S(x, t)$ $[L^2]$ is the total storage in a hillslope at time t and position x along the slope. The Darcy flux reads

$$q = -kh\left(\frac{\partial h}{\partial x}\cos i(x) + \sin i(x)\right) \tag{18}$$

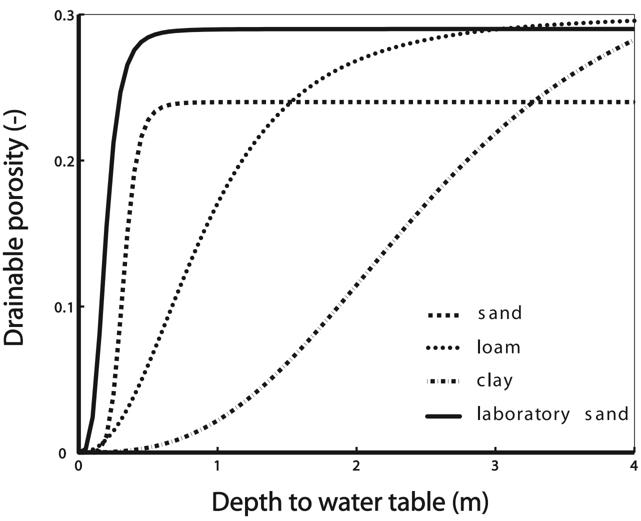

Figure 3. The relation between drainable porosity f and the depth to the water table under the assumption of hydrostatic pressure head conditions for four different soil types. The corresponding parameter values are given in Table 1.

Table 1. Van Genuchten Parameters (Regular and Modified) for Sand, Loam, Clay, and the Laboratory Sand

Parameter	Sand	Loam	Clay	Laboratory Sand
		Regular[a]		
θ_s	0.26	0.37	0.47	0.32
θ_r	0.01	0.05	0.16	0.05
α, 1/cm	−0.0324	−0.0161	−0.0066	−0.0630
n	6.6600	2.6632	1.8601	4.4545
		Modified[b]		
θ_s	0.26	0.38	0.48	0.32
θ_r	0.01	0.06	0.19	0.05
α, 1/cm	−0.0301	−0.0090	−0.0020	−0.0532
n	5.9940	1.7608	1.1830	3.7708

[a]For regular, $\mathbf{m = 1 - 1/n}$.
[b]For modified, $\mathbf{m = 1 + 1/n}$.

where k $[LT^{-1}]$ is the hydraulic conductivity. The storage S is defined as [*Fan and Bras*, 1998; *Troch et al.*, 2003]

$$S = \gamma wh \tag{19}$$

where $\gamma = \gamma(x, t)$ (dimensionless) can be regarded as the specific yield according to the definition of *Bear* [1972] and is defined as

$$\gamma = \frac{1}{h}\int_{h=0}^{h} f\,\mathrm{d}h \tag{20}$$

which by using (15) can also be expressed as:

$$\gamma = \frac{1}{h}\int_{h=0}^{h} \mathrm{d}s = \frac{s(h) - s(0)}{h} \tag{21}$$

Note that in the given context the term specific yield (γ) represents a porosity, whereas drainable porosity is actually a storage coefficient. Note also that for a constant drainable porosity, f and γ have the same value. Substitution of (19), (20), and (21) into (17) yields

$$wf\frac{\partial h}{\partial t} = -\frac{\partial\{wq\}}{\partial x} + Nw \tag{22}$$

or

$$\frac{\partial h}{\partial t} = -\frac{1}{wf}\frac{\partial\{wq\}}{\partial x} + \frac{N}{f} \tag{23}$$

which is the governing equation for the HSB model [*Troch et al.*, 2003]. Note that the parameter f is now a function of h. Equation (23) may be expanded, using (18), into [*Hilberts et al.*, 2004]

$$\frac{\partial(wq)}{\partial x} = -\left\{kw\frac{\partial h}{\partial x} + kh\frac{\partial w}{\partial x}\right\}\left\{\frac{\partial h}{\partial x}\cos i(x) + \sin i(x)\right\} - kwh\left\{\frac{\partial^2 h}{\partial x^2}\cos i(x) - \frac{\partial h}{\partial x}\frac{\partial i(x)}{\partial x}\sin i(x) + \frac{\partial i(x)}{\partial x}\cos i(x)\right\} \tag{24}$$

Upon substitution of (16) and (24) in (23) we obtain an expression for $\partial h/\partial t$ that is explicit in h and that reads

$$\begin{aligned}\frac{\partial h}{\partial t} = &\frac{1}{(\theta_s-\theta_r)\left\{1-\left(1+\left(\alpha\left(\frac{h-D}{\cos(i)}\right)\right)^n\right)^{-\left(\frac{n+1}{n}\right)}\right\}} \\ &\cdot\left\{N+\frac{1}{w}\left\{\left\{kw\frac{\partial h}{\partial x}+kh\frac{\partial w}{\partial x}\right\}\left\{\frac{\partial h}{\partial x}\cos i(x)+\sin i(x)\right\}\right\}\right\} \\ &+\frac{1}{(\theta_s-\theta_r)\left\{1-\left(1+\left(\alpha\left(\frac{h-D}{\cos(i)}\right)\right)^n\right)^{-\left(\frac{n+1}{n}\right)}\right\}} \\ &\cdot\left\{kh\left\{\frac{\partial^2 h}{\partial x^2}\cos i(x)-\frac{\partial h}{\partial x}\frac{\partial i(x)}{\partial x}\sin i(x)+\frac{\partial i(x)}{\partial x}\cos i(x)\right\}\right\}\end{aligned} \tag{25}$$

The outflow from the hillslope is calculated using the mass conservative scheme:

$$Q(t)=\int_{x=0}^{L}\left(-wf\frac{\partial h}{\partial t}+Nw\right)\mathrm{d}x \tag{26}$$

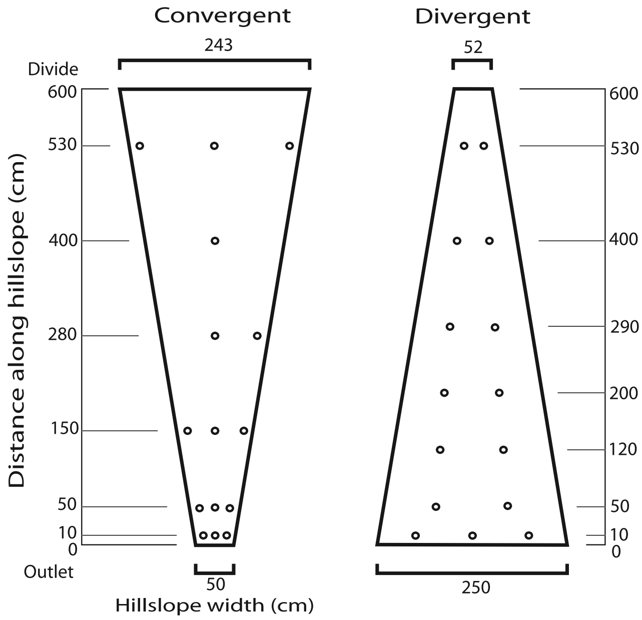

Figure 4. Plan view of the convergent and divergent laboratory slopes and the position of the piezometers (indicated by small circles).

4. Experimental Setup

4.1. Laboratory Hillslopes and the Drainage Experiment

[14] The concept of storage-dependent drainable porosity is analyzed by comparing the results of the HSB model to measurements of water tables and outflow rates from a drainage experiment in a laboratory setup. The experiments are conducted for two distinct hillslope configurations: linear convergent and linear divergent. A constant and uniform rainfall rate is applied by a rainfall generator to both the convergent and divergent hillslope, until a steady state water table is reached. Then the rainfall generator is stopped and from this steady state initial condition the drainage experiment is started. For each hillslope shape we investigate the hydrological response for 5%, 10%, and 15% bedrock slope. The two hillslopes, their dimensions, and the location of the piezometers on the slopes are shown in Figure 4. Two versions of the HSB model will be evaluated: the original HSB model, where drainable porosity and conductivity are constant, and the revised, more general HSB model where drainable porosity is a state-dependent parameter, calculated according to (16).

[15] Both HSB models are first run in an uncalibrated mode with the hydraulic conductivity k set to the value that was measured on a core sample in the laboratory, and for the original HSB model the drainable porosity is set to $\theta_s - \theta_r$. In the second experiment the two models are run in a fully calibrated mode. The methods used to determine the parameter values for the two models are described in Sections 4.3 and 4.4.

4.2. Boundary Conditions

[16] All sides of the hillslope, except the outlet and the soil surface, are made impermeable by means of plastic sheets. At the outlet a highly permeable filter is placed at 0.05 m above the "bedrock," for a total height of 0.20 m. The outlet is thus subject to a Dirichlet-type boundary condition, with the pressure head set to 0.05 m.

[17] Every 24 seconds automated water table readings are obtained from the piezometers. All piezometers are connected to a Campbell data logger with a multiplexer. Outflow rates are measured every minute using a calibrated vessel with a floating device. To reduce the noise in the signals, the water table readings are averaged over 2-min intervals and the outflow rates over 10-min intervals.

4.3. Parameterization of the Revised HSB Model

[18] For the revised HSB model, the drainable porosity is calculated using (16), which is parameterized using the relationship $m = 1 + 1/n$ to determine the van Genuchten parameter values for the coarse sand used in the laboratory experiment. We will hereafter refer to these parameters as the modified van Genuchten parameters, whereas the parameters that are optimized using the regular relationship $m = 1 - 1/n$ will be referred to as the regular van Genuchten parameters. They are given in Table 1. The retention curves fitted to the measurements are plotted in Figure 5. The soil depth (D) was measured separately for each hillslope shape and is given in Table 2. Because the laboratory bedrock has a negligible leakage and vertical fluxes in the unsaturated zone are assumed to be 0, the sink/source term N is set to 0 for all simulations.

[19] In the uncalibrated runs the hydraulic conductivity k is set to 40 m/d, which is the value that was measured on a laboratory core sample. In the calibrated runs the conductivity is the only fitting parameter in this version of the model, and it is optimized by minimizing the summed absolute difference between measured and modelled outflow rates (i.e., the 1-norm). The calibrated value is given in Table 2.

4.4. Parameterization of the Original HSB Model

[20] In the uncalibrated runs the hydraulic conductivity k is set to 40 m/d as above. The value for drainable porosity is set to $(\theta_s - \theta_r)$, which seems the most suitable value for an a

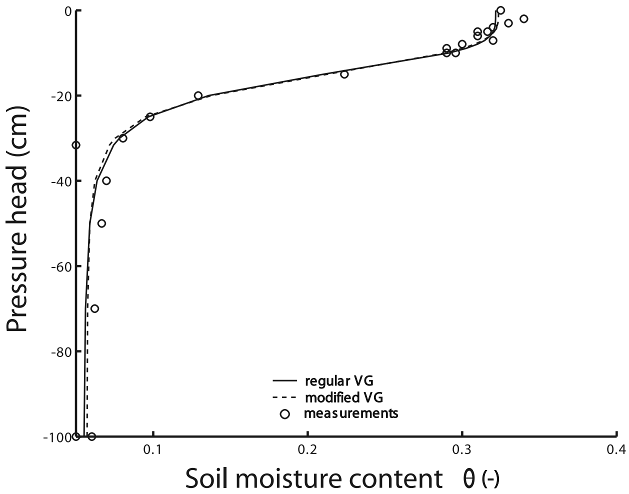

Figure 5. The retention curve of the sandy soil used in the laboratory experiments. Circles indicate measurements, the solid line depicts the regular van Genuchten curve, and the dashed line depicts the modified van Genuchten curve.

priori estimate, since we expect the aquifer to reach full gravitational drainage under the assumptions of Dupuit-Forchheimer. In the calibrated runs the parameters of the original HSB model are both regarded as fitting parameters. The drainable porosity is calculated as [*Paniconi et al.*, 2003]

$$\gamma' = \frac{V_c}{V_i} \tag{27}$$

where V_c is the cumulative outflow from the laboratory drainage experiment, and V_i is the volume of soil (pore space plus solid matrix) occupied by the water in the saturated zone at time zero. Note that based on the definitions given in Section 1, γ' is better described as the specific yield [*Johnson*, 1967; *Bear*, 1972] of the aquifer under study, and it can be regarded as an estimate for γ as given in (20). Note also that for a constant value for f (as was assumed by *Troch et al.* [2003], *Paniconi et al.* [2003], and *Hilberts et al.* [2004]) the three parameters collapse into the same value: $\gamma' = \gamma = f$. The calculated specific yield values are given in Table 2. The optimal value for conductivity is then found by minimizing the 1-norm of the difference between measured and modelled outflow rates. The optimal parameter values are also given in Table 2.

4.5. Parameter Interpretation

[21] The revised HSB model has four additional unsaturated zone parameters: θ_s, θ_r, α, and n compared to one (γ') in the original HSB model. These four modified van Genuchten parameters are all determined a priori on the basis of soil water retention characteristics (which can be derived for most soil types using pedotransfer functions or are otherwise relatively easy to estimate from soil core samples). The original HSB model involves the parameter specific yield (γ'), which can be calculated a posteriori on the basis of hydrographs and initial groundwater storage. As stated in the introduction of this paper, the value of drainable porosity (or specific yield in the case of the original HSB model) is not unique for a given soil or hillslope. As is apparent from Table 2, it will vary with slope angle and plan shape of the hillslope, and with other factors as well (profile shape, initial water table level and moisture status, etc.). Using the modified van Genuchten parameterization to describe the drainable porosity removes a parameter from the model that has a poor physical basis (γ'), and replaces it with a storage-dependent parameter that is clearly physically defined (f) and that does not need to be calibrated on outflow data and piezometric measurements, but instead can be calculated based on the soil water retention characteristics (measured a priori) and the simulated depth to the water table. Thus our approach has potential for hydrological analysis in ungauged basins.

5. Results

5.1. Uncalibrated Models

[22] The outflow of the original HSB model, the revised HSB model, and laboratory measurements are shown in Figure 6. Note that the y axis is scaled differently for the different bedrock slope angles. Figure 6 shows that the convergent hillslopes drain more slowly than the divergent ones, which is primarily caused by a smaller outlet width [*Troch et al.*, 2003]. Furthermore we notice that for the 5% slopes the fluxes for the original HSB model are clearly overestimated, especially for the convergent slope. The revised HSB model shows a much better fit. For the 10% convergent hillslope we notice that the original HSB model has an almost perfect fit, whereas the revised HSB model slightly underestimates the fluxes at early times and overestimates for large times. For the 10% divergent slope both models show a good fit to the data. For the 15% convergent slope the revised HSB model again underestimates the fluxes at early times and slightly overestimates for large times. The original HSB model displays the same pattern, although the underestimation at early times is smaller and the overestimation for large times is larger. For the 15% divergent slope, both models show slightly underestimated fluxes.

[23] In Figure 7 the water table profiles are plotted for the six hillslope configurations at times 0, 60, 120, and

Table 2. Calibrated Conductivity Values k (m/d) for the Original and Revised HSB Model, Specific Yield (γ') Values, and Soil Depth D (m) for All Six Hillslope Configurations

	Original HSB						Revised HSB			
	k 5%	k 10%	k 15%	γ' 5%	γ' 10%	γ' 15%	k 5%	k 10%	k 15%	All HSB D
Convergent	35	40	43	0.12	0.18	0.23	44	49	56	0.48
Divergent	30	29	31	0.18	0.26	0.31	32	34	31	0.44

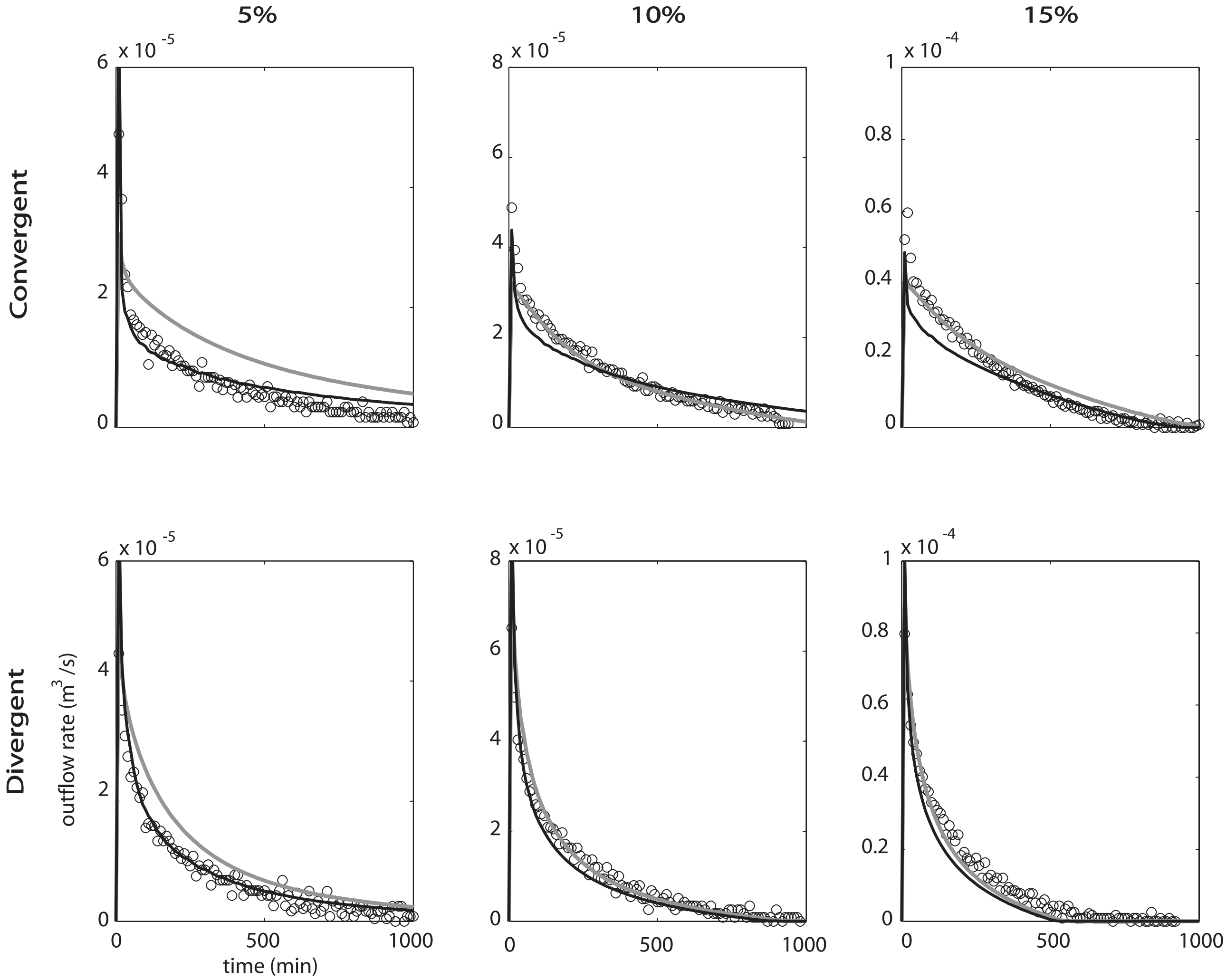

Figure 6. Outflow rates for the uncalibrated HSB models for the six hillslope configurations. Measured values are shown as circles, the original HSB model is the shaded line, and the revised HSB model is the solid line.

300 min. The initial conditions (which are steady state profiles as a result of the applied rainfall) show higher saturation degrees on the upper parts of the three convergent slopes when compared to the divergent ones, due to the difference in outflow width. We notice that the original HSB model systematically overestimates the water table height for all slope shapes and all bedrock slope angles, especially at early times. The revised HSB model is clearly more accurate, even though it still overestimates the water table values. The improvement of the revised HSB model is most evident at early times, when a low value for the drainable porosity in the revised HSB model causes the water tables to drop relatively quickly. For large times the simulated water table profiles for the two models converge.

5.2. Calibrated Models

[24] Table 2 gives the optimized conductivity values for both models and the calibrated specific yield values for the original HSB model. Figure 8 shows the outflow of the original HSB model, the revised HSB model, and laboratory measurements. Figure 9 shows the evolution of the space-averaged drainable porosity value as function of time for the revised model.

[25] The specific yield value increases for steeper slopes, as expected since less water is retained in the unsaturated zone on steep hillslopes, due to increased gravitational drainage. The relatively low values for the 5% hillslopes explain the large overestimation of the uncalibrated original HSB model on these hillslopes in Figure 6. Noteworthy is that the specific yield value for the 15% divergent slope ($\gamma' = 0.31$) exceeds the value ($\theta_s - \theta_r$) = 0.29. This indicates that more water has drained than is estimated based on the initial saturated storage (V_i), from which we can conclude that also water from the initial unsaturated zone has drained.

[26] With regard to the optimized conductivity values, we notice that the values are slightly higher for the convergent slopes and lower for the divergent slopes when compared to the laboratory determined value of 40 m/d. This may be caused by the higher initial water table values for the convergent slopes when compared to the divergent slopes, thereby increasing the average conductivity for these slopes.

[27] Overall, we notice that compared to the hydrographs in Figure 6, the fit of both models has improved (not greatly though), as expected. The overall fit of the revised HSB model is slightly poorer compared to the original HSB model. However, at early times when the impact of capil-

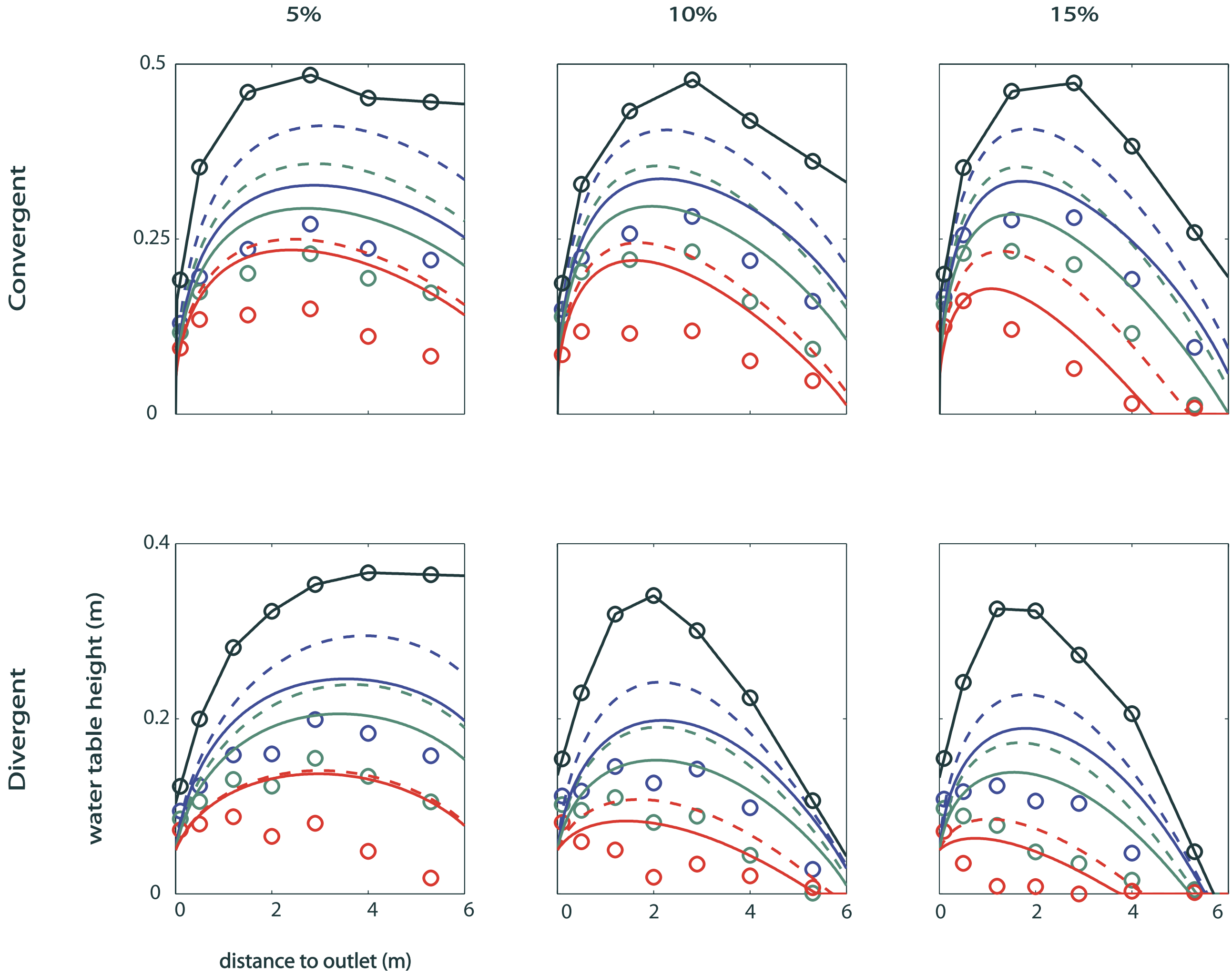

Figure 7. Water table profiles for the uncalibrated HSB models at time 0 (black), at 60 min (blue), at 120 min (green) and at 300 min (red) for the six hillslope configurations. The measured values are the circles, the original HSB model is represented by the dashed lines, and the revised HSB model is represented by the solid lines.

larity on storage and flow is highest due to high saturation degree, the fit has improved. For the 5% convergent slope we see that the match is good at the beginning of the drainage experiment, but is overestimated at large times. An improvement in the fitting of the tail part of the hydrograph is achieved at the expense of the goodness of fit at early times: the drop of the flux rate is then too sharp. The fact that this sharp decrease in modelled fluxes is not reflected in the measurements may indicate that there is some recharge from the unsaturated zone during the early stages of drainage, due to the applied rainfall just before the experiment. For the 10% slope the fit to the data is very good for small times and the overestimation for large time is small. For the 15% slope the fit to the data is good for small times, but there is underestimation of flux for large times. The 5% divergent slope shows an almost perfect fit. For the 10% and the 15% divergent slopes, the fluxes initially drop too quickly, but for larger times the fit improves. The space-averaged drainable porosity in Figure 9 shows a quick convergence toward $\theta_s - \theta_r$ for the hillslopes that drain quickly (i.e., divergent and steep slopes), and show slow convergence for slowly draining slopes. When convergence is reached, the advantages of the revised HSB model vanish, because effectively f then remains constant.

[28] It is noteworthy in this context that although the time and space averaged value of f may in some cases be (almost) equal to the value of γ', the modelled states and fluxes can be very different for the two models. A low value of f at early times causes the water tables to drop quickly (and fastest where the water tables are closest to the surface), thereby changing the water table profiles fundamentally from the original HSB model. Even when the values of f and γ' are equal afterward, the outflow behavior and water table dynamics remain different for the two models. The opposite effect can also be noticed: the averaged value of f and the value of γ' can in some cases be different, whereas the modelled outflow for both models can be almost indistinguishable. This effect can for example be seen in Figure 8 for the 5% divergent slope, where the time and space averaged value of drainable porosity is equal to f = 0.25, and for the original HSB model γ' = 0.18, whereas the modelled outflow is very much alike.

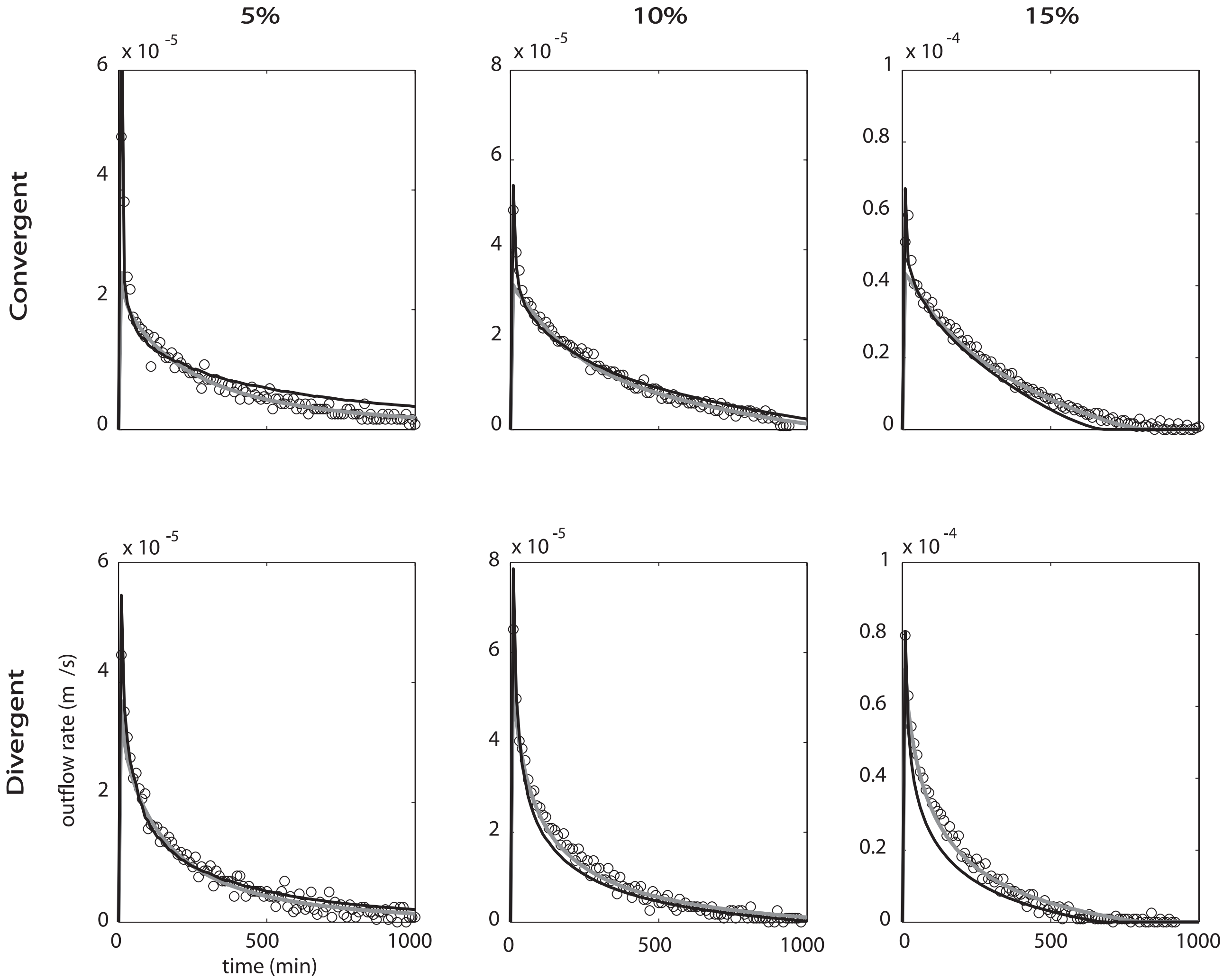

Figure 8. Outflow rates for the calibrated HSB models for the six hillslope configurations. Measured values are shown as circles, the original HSB model is the shaded line, and the revised HSB model is the solid line.

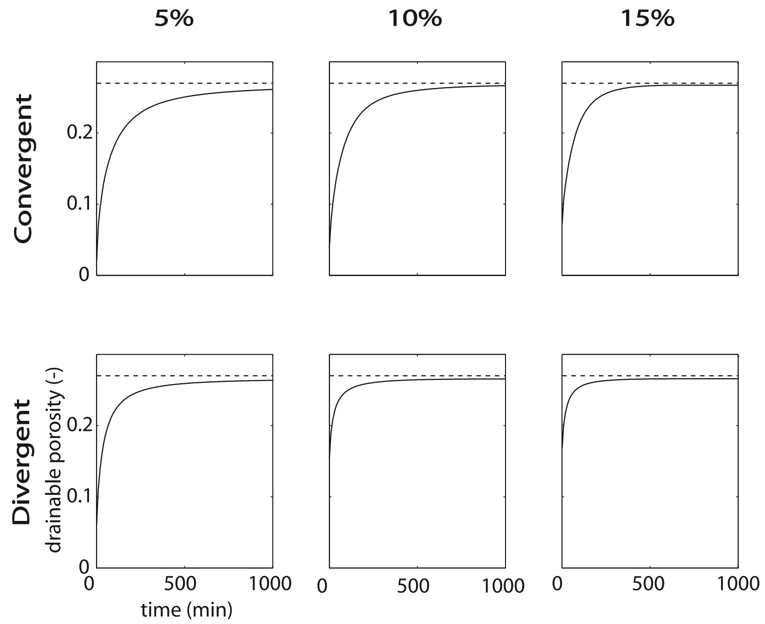

Figure 9. Space-averaged drainable porosity values for the calibrated revised HSB models for the six hillslope configurations. The dashed line indicates the value $(\theta_s - \theta_r)$.

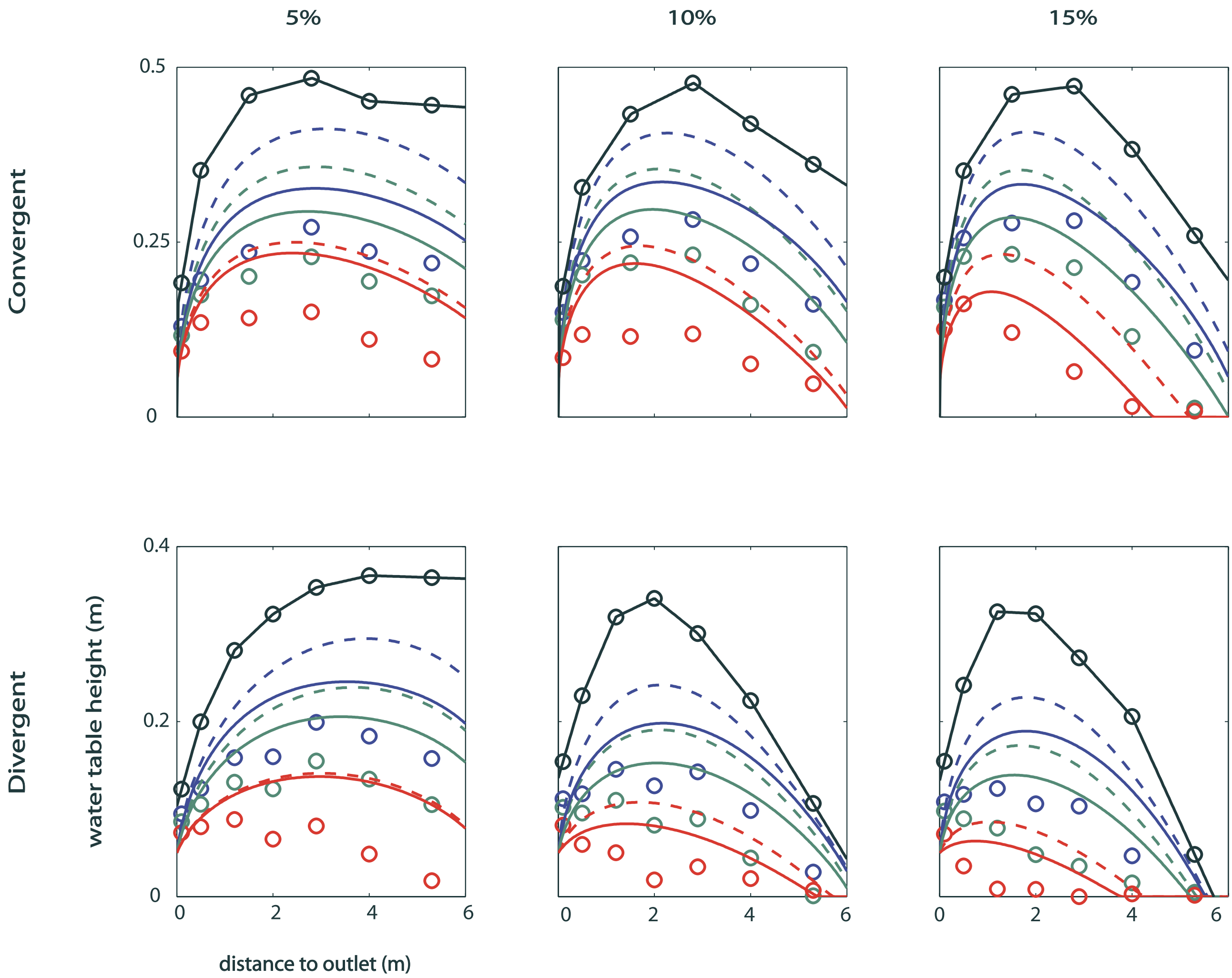

Figure 10. Water table profiles for the calibrated HSB models at time 0 (black), at 60 min (blue), at 120 min (green), and at 300 min (red) for the six hillslope configurations. The measured values are the circles, the original HSB model is represented by the dashed lines, and the revised HSB model is represented by the solid lines.

[29] In Figure 10 the water table profiles are plotted for the six hillslope configurations at times 0, 60, 120, and 300 min. As in Figure 6, we notice that both models overestimate the water table values. Once again the revised HSB model is clearly more accurate. However, due to the calibration of the original HSB model (i.e., the lower values of specific yield), the differences between both models have decreased slightly although the differences between the original and revised HSB models for early times still range up to 0.10 m.

6. Discussion and Conclusions

[30] In this paper we have presented, for horizontal and sloping bedrock aquifers, an analytical expression for storage-dependent drainable porosity (for horizontal and sloping bedrock), thereby incorporating some of the effects of the unsaturated zone on groundwater storage and fluxes. The assumption underlying the derivation is that during drainage the pressure head in the unsaturated zone is permanently in vertical hydraulic equilibrium. The derived expressions (i.e., (12) and (16)) link drainable porosity directly to the depth to the water table, thereby transforming it from a fitting parameter into a state-dependent parameter. The derived expression is then incorporated into the HSB model and compared (in terms of water table height and outflow values) to the results of the original (constant f) HSB model and to a series of laboratory measurements. The validation of the model is conducted on a convergent and a divergent hillslope, for 5%, 10%, and 15% bedrock slope inclination (i.e., 6 different hillslope configurations). Two simulation settings were analyzed: an uncalibrated model run, where the model parameters were determined based on conductivity and water retention measurements on soil cores; and a fully calibrated run, where the optimized parameter values (i.e., specific yield and conductivity in the case of the original HSB and only conductivity in the case of the revised HSB) were used.

[31] The comparison of the HSB models to the measurements from the laboratory hillslopes shows that it is possible to capture the general features of a drainage experiment using either one of the HSB models. Overall the original HSB model (having one fitting parameter more than the revised HSB model) shows a slightly better fit on the

hydrographs when compared to the revised HSB model. The peak outflow values however (the first few minutes after initiation of the experiments) are better captured by the revised HSB model. The revised HSB model's performance in simulating water table movements is much more accurate than that of the original HSB model. The improved match of the revised HSB model to piezometric measurements is worth stressing because the ability to model water tables is a key attribute of the model, making it possible to investigate phenomena such as saturation excess runoff.

[32] The difference between the original and the revised HSB model performance on outflow results is most clearly visible for the uncalibrated model runs on gentle slopes: the large overestimation of fluxes by the original HSB model here clearly advocates the calculation of f as a storage-dependent parameter. Also remarkable is the good match between the revised HSB model and outflow measurements without any calibration for the divergent slopes. The fact that the performance of the original HSB model is not independent of slope inclination and initial conditions, together with the ability of the revised model to more accurately simulate water table dynamics, clearly demonstrates the importance of regarding drainable porosity as a function of storage.

[33] A further comment on the storage-dependent drainable porosity concept worth mentioning is that even when the time and space averaged value of f is equal to the calibrated value of γ', the dynamic behavior of both models can be significantly different. A low value of f at early times can change the water table profiles such that the hydrographs for both models remain different thereafter. The opposite also holds: even when the averaged value of f and the value of γ' differ significantly, the outflow behavior may be almost identical.

[34] In relation to the hydrographs we notice that for some drainage experiments the fluxes as modelled with the revised HSB model drop too quickly at early times during drainage, although the cumulative modelled outflow is generally in accordance with the measurements. Since changing the van Genuchten parameters would influence the cumulative volumes, one can conclude that for the revised HSB model it is not possible to obtain a better fit for the hydrographs by tuning these parameters. This leads to the conclusion that in the early stages of our drainage experiments, the assumptions underlying the drainable porosity expression might not be completely valid. Since the experiment is started right after a rainfall event, it is probable that there is still some vertical downward flux in the unsaturated zone, violating our assumption of zero recharge and hydraulic equilibrium in the unsaturated zone.

[35] *Vachaud and Vauclin* [1975] concluded that the capillary fringe plays an important role in the flow of water. Incorporating the capillary fringe as an integral part of the Boussinesq aquifer (i.e., substituting h by $h + \psi_c$, where ψ_c is the capillary fringe) will not affect the outflow behavior of the HSB model, but will improve the simulated water tables. The substitution effectively implies changing from the assumption that transport only occurs below the water table (underlying Boussinesq-type models) into the assumption that transport only takes place in the saturated zone.

[36] Ongoing work is aimed at generalizing the expression for drainable porosity such that it can be calculated as a storage-dependent parameter in case of nonzero steady state fluxes in the unsaturated zone. Analytical integration of the corresponding soil moisture profiles is then not possible, but semianalytical solutions may be derived by means of piecewise integration of the soil hydraulic characteristics [see *Rockhold et al.*, 1997]. In the case of nonzero recharge we may also have to consider hysteresis phenomena in the soil water retention characteristic. It is expected that a more general expression would improve the revised HSB model's performance, especially just after initiation of the drainage experiments. Moreover, it would enable us to extend the analysis of the concept of storage-dependent drainable porosity to recharge scenarios, rendering the revised HSB model suitable for rainfall-runoff simulations in poorly gauged catchments. Future work will also evaluate these concepts by comparison to a three-dimensional Richards equation based model and to field data.

[37] **Acknowledgments.** This work has been supported in part by Delft Cluster (project DC-030604). The authors also wish to thank A. van Loon and E. van Rijsselt for their help in collecting the laboratory data.

References

Abdul, A., and R. Gillham (1989), Field studies on the effects of the capillary fringe on streamflow generation, *J. Hydrol.*, *112*, 1–18.
Bear, J. (1972), *Dynamics of Fluids in Porous Media*, Elsevier, New York.
Beven, K. (1981), Kinematic subsurface stormflow, *Water Resour. Res.*, *17*, 1419–1424.
Bierkens, M. (1998), Modeling water table fluctuations by means of a stochastic differential equation, *Water Resour. Res.*, *34*, 2485–2499.
Boussinesq, J. (1877), Essai sur la theorie des eaux courantes, *Mem. Acad. Sci. Inst. Fr.*, *23*, 680 pp.
Childs, E. (1971), Drainage of groundwater resting on a sloping bed, *Water Resour. Res.*, *7*, 1256–1263.
Dingman, S. (2002), *Physical Hydrology*, Prentice-Hall, Upper Saddle River, N. J.
Duffy, C. (1996), A two-state integral-balance model for soil moisture and groundwater dynamics in complex terrain, *Water Resour. Res.*, *32*, 2421–2434.
Fan, Y., and R. Bras (1998), Analytical solutions to hillslope subsurface storm flow and saturated overland flow, *Water Resour. Res.*, *34*, 921–927.
Fink, J., J.-Y. Parlange, and A. El-Kadi (2001), One last visit to the capillarity correction for free surface flow, *Water Resour. Res.*, *37*, 827–829.
Freeze, R., and J. Cherry (1979), *Groundwater*, Prentice-Hall, Upper Saddle River, N. J.
Gillham, R. (1984), The capillary fringe and its effect on water-table response, *J. Hydrol.*, *67*, 307–324.
Heidari, M., and A. Moench (1997), Evaluation of unconfined-aquifer parameters from pumping test data by nonlinear least squares, *J. Hydrol.*, *192*, 300–313.
Hilberts, A., E. van Loon, P. Troch, and C. Paniconi (2004), The hillslope-storage Boussinesq model for spatially variable bedrock slope, *J. Hydrol.*, *291*, 160–173.
Hillel, D. (1980), *Applications of Soil Physics*, Elsevier, New York.
Hogarth, W. L., J.-Y. Parlange, M. B. Parlange, and D. Lockington (1999), Approximate analytical solution of the Boussinesq equation with numerical validation, *Water Resour. Res.*, *35*, 3193–3197.
Johnson, A. (1967), Specific yield—Compilation of specific yields for various materials, *U.S. Geol. Surv. Water Supply Pap.*, *1662-D*.
Kim, C., and M. Bierkens (1995), A formula for computation of time-varying recharge of ground water—Comment, *J. Hydrol.*, *171*, 191–193.
Luthin, J. (1966), *Drainage Engineering*, John Wiley, Hoboken, N. J.
Moench, A. (1994), Specific yield as determined by type-curve analysis of aquifer-test data, *Ground Water*, *32*(6), 949–957.
Moench, A. (2003), Estimation of hectare-scale soil-moisture characteristics from aquifer-test data, *J. Hydrol.*, *281*, 82–95.
Nachabe, M. (2002), Analytical expressions for transient specific yield and shallow water table drainage, *Water Resour. Res.*, *38*(10), 1193, doi:10.1029/2001WR001071.
Neuman, S. (1987), On methods of determining specific yield, *Ground Water*, *25*(6), 679–684.

Nielsen, P., and P. Perrochet (2000), Watertable dynamics under capillary fringes: Experiments and modelling, *Adv. Water Resour.*, *23*, 503–515.
Nwankwor, G., R. Gillham, G. van der Kamp, and F. Akindunni (1992), Unsaturated and saturated flow in response to pumping of an unconfined aquifer: Field evidence of delayed drainage, *Ground Water*, *30*(5), 690–700.
Ogden, F., and B. Watts (2000), Saturated area formation on nonconvergent hillslope topography with shallow soils: A numerical investigation, *Water Resour. Res.*, *36*, 1795–1804.
Paniconi, C., P. Troch, E. van Loon, and A. Hilberts (2003), The hillslope-storage Boussinesq model for subsurface flow and variable source areas along complex hillslopes: 2. Intercomparison with a three-dimensional Richards equation model, *Water Resour. Res.*, *39*(11), 1317, doi:10.1029/2002WR001730.
Parlange, J. Y., and W. Brutsaert (1987), A capillarity correction for free surface flow of groundwater, *Water Resour. Res.*, *23*, 805–808.
Parlange, J. Y., W. Brutsaert, J. Fink, and A. El-Kadi (1990), A capillarity correction for free surface flow revisited, *Water Resour. Res.*, *26*, 1691–1692.
Parlange, J. Y., F. Stagnitti, A. Heilig, J. Szilagyi, M. B. Parlange, T. S. Steenhuis, W. L. Hogarth, D. A. Barry, and L. Li (2001), Sudden draw-down and drainage of a horizontal aquifer, *Water Resour. Res.*, *37*, 2097–2101.
Richards, L. (1931), Capillary conduction of liquids through porous mediums, *Physics*, *1*, 318–333.
Rockhold, M., C. Simmons, and M. Fayer (1997), An analytical solution technique for one-dimensional, steady vertical water flow in layered soils, *Water Resour. Res.*, *33*, 897–902.
Stagnitti, F., M. B. Parlange, T. S. Steenhuis, and J.-Y. Parlange (1986), Drainage from a uniform soil layer on a hillslope, *Water Resour. Res.*, *22*, 631–634.
Su, N. (1994), A formula for computation of time-varying recharge of groundwater, *J. Hydrol.*, *160*, 123–135.
Szilagyi, J. (2004), Vadose zone influences on aquifer parameter estimates of saturated-zone hydraulic theory, *J. Hydrol.*, *286*, 78–86.
Tritscher, P., W. Read, and P. Broadbridge (2000), Specific yield for a two-dimensional flow, *Water Resour. Res.*, *36*, 1393–1402.
Troch, P. (1992), Conceptual basin-scale runoff process models for humid catchments: Analysis, synthesis and applications, Ph.D. thesis, Ghent Univ., Ghent, Netherlands.
Troch, P., E. van Loon, and A. Hilberts (2002), Analytical solutions to a hillslope-storage kinematic wave equation for subsurface flow, *Adv. Water Resour.*, *25*, 637–649.
Troch, P., C. Paniconi, and E. van Loon (2003), The hillslope-storage Boussinesq model for subsurface flow and variable source areas along complex hillslopes: 1. Formulation and characteristic response, *Water Resour. Res.*, *39*(11), 1316, doi:10.1029/2002WR001728.
Troch, P., A. van Loon, and A. Hilberts (2004), Analytical solution of the linearized hillslope-storage Boussinesq equation for exponential hillslope width functions, *Water Resour. Res.*, *40*, W08601, doi:10.1029/2003WR002850.
Vachaud, G., and M. Vauclin (1975), Comment on "A numerical model based on coupled one-dimensional Richards and boussinesq equations" by Mary F. Pikul, Robert L. Street, and Irwin Remson, *Water Resour. Res.*, *11*, 506–509.
van Genuchten, M. (1980), A closed-form equation for predicting the hydraulic conductivity of unsaturated soils, *Soil Sci. Am. J.*, *44*, 892–898.
Walter, M., J.-S. Kim, T. Steenhuis, J.-Y. Parlange, A. Heilig, R. Braddock, J. Selker, and J. Boll (2000), Funneled flow mechanisms in a sloping layered soil: Laboratory investigation, *Water Resour. Res.*, *36*, 841–849.
Weiler, M., and J. McDonnell (2004), Virtual experiments: A new approach for improving process conceptualization in hillslope hydrology, *J. Hydrol.*, *285*, 3–18.
Woods, R., M. Sivapalan, and J. Robinson (1997), Modeling the spatial variability of subsurface runoff using topographic index, *Water Resour. Res.*, *33*, 1061–1073.
Zecharias, Y., and W. Brutsaert (1988), Recession characteristics of groundwater outflow and base flow from mountainous watersheds, *Water Resour. Res.*, *24*, 1651–1658.

A. G. J. Hilberts and P. A. Troch, Hydrology and Quantitative Water Management Group, Department of Environmental Sciences, Wageningen University, Nieuwe Kanaal 11, 6709 PA Wageningen, Netherlands. (arno.hilberts@wur.nl; peter.troch@wur.nl)

C. Paniconi, Institut National de la Recherche Scientifique, Centre Eau, Terre et Environnement, Université du Québec, 490 de la Couronne, Quebec, QC, Canada G1K 9A9. (claudio_paniconi@ete.inrs.ca)